Current Biology, Vol. 15, 1899–1911, November 8, 2005, ©2005 Elsevier Ltd All rights reserved. DOI 10.1016/j.cub.2005.09.052

Patterns of Auxin Transport and Gene Expression during Primordium Development Revealed by Live Imaging of the *Arabidopsis* Inflorescence Meristem

Marcus G. Heisler, Carolyn Ohno, Pradeep Das, Patrick Sieber, Gonehal V. Reddy, Jeff A. Long, and Elliot M. Meyerowitz*
Division of Biology
California Institute of Technology
Pasadena, California 91125

Summary

Background: Plants produce leaf and flower primordia from a specialized tissue called the shoot apical meristem (SAM). Genetic studies have identified a large number of genes that affect various aspects of primordium development including positioning, growth, and differentiation. So far, however, a detailed understanding of the spatio-temporal sequence of events leading to primordium development has not been established.
Results: We use confocal imaging of green fluorescent protein (GFP) reporter genes in living plants to monitor the expression patterns of multiple proteins and genes involved in flower primordial developmental processes. By monitoring the expression and polarity of PINFORMED1 (PIN1), the auxin efflux facilitator, and the expression of the auxin-responsive reporter DR5, we reveal stereotypical PIN1 polarity changes which, together with auxin induction experiments, suggest that cycles of auxin build-up and depletion accompany, and may direct, different stages of primordium development. Imaging of multiple GFP-protein fusions shows that these dynamics also correlate with the specification of primordial boundary domains, organ polarity axes, and the sites of floral meristem initiation.
Conclusions: These results provide new insight into auxin transport dynamics during primordial positioning and suggest a role for auxin transport in influencing primordial cell type.

Introduction

Primordium development is a fundamental process in plants and animals. It involves a positioning mechanism that defines where the tissue or organ will arise as well as changes to growth and differentiation that result in outgrowth and the correct patterning of cell types. Lateral primordia in plants, unlike animals, initiate continuously and at regular positions from the growing tip or SAM, implying that the positioning mechanism is a dynamic and potentially self-regulating system. Recently it has been shown that the plant hormone auxin acts centrally in this process. Plants genetically or chemically impaired in their ability to transport auxin fail to form floral primordia [1]. However, externally applied auxin can rescue this defect in a position-specific manner, suggesting that the distribution of auxin in the meristem flank may determine where primordia arise [2]. Consistent with this proposal is the finding that, in the epidermis below initiating primordia, the subcellular localization of the putative auxin efflux carrier PIN1 is polarized apically, suggesting auxin is transported toward primordia from the stem epidermis. Within primordia, PIN1 is localized basally in the presumptive provascular cells forming a connection from the primordium to the vascular tissue of the stem [3, 4]. These and other observations have led to the proposal that auxin is transported apically in the epidermis toward developing primordia that then act as auxin sinks by transporting auxin into the provascular tissues, thereby depleting auxin from surrounding cells. Since auxin acts to trigger primordium development, new primordia are initiated where auxin levels are highest, that is, at a location furthest from the previous zone of depletion [3, 5].

Once primordia are positioned, boundaries are established, and cell types that result in proper organ development are specified. Genetic analysis has uncovered a large number of genes involved in these processes. The *SHOOTMERISTEMLESS* (*STM*) gene is required for SAM formation and maintenance, and its activity is necessary to keep cells in an undifferentiated state [6]. During primordium specification, *STM* is locally downregulated, and this downregulation seems to be required for differentiation to take place [7, 8]. The *CUP-SHAPED COTYLEDON* (*CUC*) genes *CUC1*, *CUC2*, and *CUC3* are required to demarcate primordium boundaries as well as promote meristem formation [9–11]. In plants mutant for all three genes, cotyledons are frequently fused and the SAM can fail to develop [10]. Genetic studies have also identified a number of genes involved in adaxial/abaxial patterning including adaxially expressed members of the class III HD-ZIP gene family such as *REVOLUTA* (*REV*) [12–14] as well as the abaxially expressed *YABBY* transcription factors such as *FILAMENTOUS FLOWER* (*FIL*) [15–17], *KANADI* genes [14, 18, 19], and miRNAs 165 and 166 [20]. In general, adaxial and abaxial factors are thought to act antagonistically to set up mutually exclusive expression domains on either side of the adaxial/abaxial boundary. However, the mechanism by which the boundary is positioned is unknown, as is the mechanism specifying the stereotypical asymmetry across this boundary, although it is proposed to correspond to a prepattern of signal emanating from the center of the meristem [12, 21].

Although we know of many genes involved in various aspects of primordial development, as discussed above, we have very little knowledge of either their temporal order of expression or how their dynamic expression domains are spatially related to one another. Furthermore, when gene function is perturbed, previously we have not been able to examine, at high temporal and spatial resolution, whether a given phenotype is a direct or indirect consequence. These types of data are now becoming available through the development of confocal imaging techniques and the use of GFP. Live imaging of *Arabidopsis* meristem cells recently enabled an analysis of cell fate and division patterns [22] as well as an analysis of the effects of various drugs that affect

*Correspondence: meyerow@caltech.edu

cell division parameters or meristem differentiation patterns [23]. With the development of GFP-spectral variants and spectral analysis, our abilities are enhanced further by enabling us to document multiple events at subcellular resolution simultaneously [24]. In this study, we take advantage of these techniques to investigate patterns of PIN1 activity and other gene and protein expression patterns. We find that PIN1 undergoes cycles of activity that not only give new insight into auxin transport dynamics during primordium establishment but also enable us to relate these dynamics to cell-type patterning during early primordial development in the inflorescence meristem.

Results

PIN1 Undergoes Cyclic Changes in Polarity and Expression

Previous work has indicated that primordium positioning is mediated by localized auxin concentrations that are in turn patterned by the activity of the auxin efflux mediator PIN1 [1, 3, 4, 25, 26]. In the meristem, the PIN1 protein is expressed predominantly in the epidermis and provasculature. In cells located in the vicinity of incipient primordia, PIN1 protein is localized laterally in the plasma membranes closest to sites of subsequent primordial emergence [3]. To investigate PIN1 dynamics, we used confocal-based live imaging of a functional *pPIN1::PIN1-GFP* fusion protein. We assessed PIN1 polarity by identifying arcs of signal in low-resolution images that we found, by analysis at high resolution, to correspond to signal within cell corners (Figure S1) and therefore to indicate the direction of auxin efflux.

Overall, our observed pattern of *pPIN1::PIN1-GFP* expression and polarity resembles previous immunological results [3], except that we find striking patterns of PIN1 polarity and expression throughout the meristem epidermis that change according to the stage of primordial development occurring at different positions. For convenience, we use "P" to designate primordia that have clearly grown out from the meristem, while "I" designates incipient primordia (assessed by position) before the onset of rapid growth. Both primordia and incipient primordia are numbered in order of appearance, with P_1 designating the youngest primordium and I_1 designating the oldest incipient primordium. From examining *pPIN1::PIN1-GFP* expression and polarity in primordia of different ages in multiple plants, a stereotypical pattern of activity can be discerned (Figure 1A; rotated and enlarged views of Figure 1A are shown in Figures 1D–1K, 1M, and 1O). Before an incipient primordium is first marked by *pPIN1::PIN1-GFP* expression, polarity at this location (I_4 in Figures 1D and 1G) is directed from one adjacent site (P_2 in Figure 1D and magnified view in Figure 1G) toward the other adjacent site (I_1 in Figures 1D and 1G). A site is first marked by relatively high levels of *pPIN1::PIN1-GFP* (I_3 in Figures 1E and 1H) when PIN1-GFP polarity is directed toward this site from both adjacent sites (P_1 and P_3 in Figures 1E and 1H). At this stage, *pPIN1::PIN1-GFP* is limited to the epidermis (compare expression at I_3 position in Figures 1A and 1C). At slightly later stages (I_2 and I_1), *pPIN1::PIN1-GFP* expression levels increase (compare positions I_2 and I_1 to I_3 in Figure 1A), and PIN1-GFP polarity becomes directed toward these sites from three adjacent primordia (P_2, P_3, and P_5 for I_1 in Figures 1F and 1I). *pPIN1::PIN1-GFP* expression in subepidermal layers also becomes detectable at these stages (positions corresponding to I_2 and I_1 in Figure 1C). As primordial growth starts to accelerate (P_1), PIN1-GFP in epidermal cells located adaxial to the primordium reverses polarity from being directed toward the primordium to being directed away from the primordium and back toward the meristem center and adjacent regions (P_1 in Figure 1J, compare to previous stage I_1 in Figure 1I). Subsequently, expression becomes reduced within the primordial epidermis (arrows in Figures 1K and 1M) but starts to reappear again by stage two of flower development [27] (arrow in Figure 1O). In subepidermal cells below the primordium, expression becomes restricted to the presumed provascular tissues (arrowheads in Figures 1L, 1N, and 1P).

To better understand changes in PIN1 expression and polarity, we conducted time-lapse confocal imaging of growing, *pPIN1::PIN1-GFP*-expressing meristems. Time-lapse images confirm the stereotypical pattern of expression build-up followed by decrease at primordial positions as well as the temporal correlation between reversals at older primordia (asterisks in Figures S2A–S2D, in the Supplemental Data available with this article online) and newly localized *pPIN1::PIN1-GFP* expression at incipient primordia (arrows in Figure S2 and Movie S1). However, we also find that *pPIN1::PIN1-GFP* expression shifts relative to the underlying cells in directions that are correlated with PIN1 polarity. After PIN1-GFP reversal, GFP signal moves from the site of reversal toward adjacent regions as well as toward the primordium tip, leaving a zone of low expression where the reversal originally took place (asterisk in Figures S2E–S2H). The adjacent regions that subsequently show increased expression correspond to sites of incipient primordia (Figures S2A–S2D and Movies S1 and S2).

These observations show that PIN1 behavior associated with flower primordium development can be divided into two phases. Initially, the establishment of PIN1 polarity toward cells destined to form an incipient primordium is correlated with a reversal in PIN1 polarity in cells surrounding an older adjacent primordium. *PIN1* expression levels then increase in cells located at the polarity focus, and this is correlated with further PIN1 reversals in adjacent primordia. The second phase is characterized by a subsequent, rapid reversal in polarity that occurs predominantly in adaxial cells surrounding the primordium. As this occurs, *pPIN1::PIN1-GFP* expression also shifts abaxially, to form a new focus of expression at the primordium tip, and adaxially, to adjacent positions destined to form new primordia.

PIN1 Polarity Changes Are Correlated with Auxin Distribution Changes

Microarray data indicating that *PIN1* may be auxin regulated in *pin1-1* meristems (within 30 min of treatment, data not shown) as well as the consistent correlation between PIN1-GFP polarity and *pPIN1::PIN1-GFP* expression level prompted us to investigate *PIN1* tran-

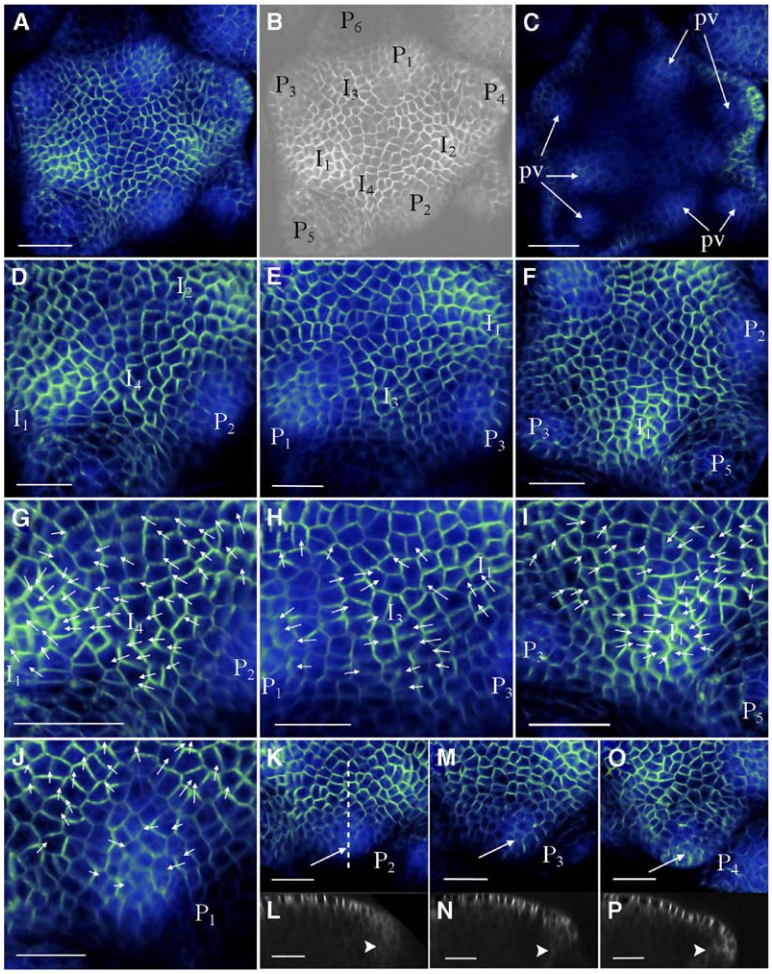

Figure 1. PIN1-GFP Expression and Polarity Patterns in the Inflorescence Meristem

(A–P) *pPIN1::PIN1-GFP* expression and polarity in a single representative meristem. In color panels, signal intensities are coded blue to yellow corresponding to increasing intensity levels, respectively. (A) View of meristem from above showing a three-dimensional volume rendering of *pPIN1::PIN1-GFP* expression and localization. (B) Identical view as in (A) indicating the numbering of primordia (P) and incipient primordia (I) with the earliest primordium marked as P_1 and later primordia as P_2–P_n. Incipient positions are labeled from the oldest I_1 to younger sites I_n. (C) View of expression below the epidermis with same orientation as in (A) and (B). Note expression in presumptive provascular tissue (pv arrows) below most positions except I_3 and I_4. (D–F) Closer views of regions surrounding I_4, I_3, and I_1, respectively. (G–J) Magnified views of cells surrounding I_4, I_3, and I_1, respectively (same orientation as [D]–[F]) showing the apparent polarity of PIN1-GFP (arrows) in cells where it could be clearly discerned. (G) There is no obvious pattern of polarity associated with position I_4. Instead, polarity in this region is predominantly directed toward I_1 and away from P_2. (H) PIN1-GFP polarity at site I_3 is directed toward I_3 from two adjacent positions, P_1 and P_3. (I) *pPIN1::PIN1-GFP* expression at I_1 is stronger compared to I_3 (compare I_1 in [F] with I_3 in [E]), and this higher expression level is coincident with PIN1-GFP polarity directed toward I_1 from three adjacent primordia, P_2, P_3, and P_5. (J) In primordium P_1, cells adaxial to the primordium show a reversed direction of polarity compared to I_1. Instead of PIN1-GFP being localized toward the primordium (as in Figure 1I), cells surrounding the primordium exhibit PIN1-GFP polarity in the direction away from the primordium, back toward the meristem and adjacent regions (arrows). (K, M, and O) Close-up views of P_2, P_3, and P_4 from (A). (L, N, and P) Reconstructed medial longitudinal sections (representative section orientation shown by dotted line in [K]) corresponding to the primordia shown in (K), (M), and (O), respectively. (K) At stage P_2, *pPIN1::PIN1-GFP* expression (arrow in [K]) appears reduced compared to P_1 and I_1. This pattern remains largely unchanged during stage P3 (arrow in [M]) until stage P4, when signal starts to reappear in this region (arrow in [O]). Below the epidermis of developing primordial, there is a gradual restriction of *pPIN1::PIN1-GFP* expression to the presumptive provasculature (arrowheads in [L], [N], and [P]). Scale bars in (A)–(C), 30 μm; in (D)–(J), (K), (M), and (O), 20 μm; and in (L), (N), and (P), 10 μm.

scription in response to auxin using quantitative real-time polymerase chain reaction (PCR). We found that treatment of dissected wild-type inflorescences with 100 μM indole-3-acetic acid (IAA) resulted in *PIN1* expression levels increasing by a factor of 2.3 (2.2–2.3) after 60 min (Figure 2A). A stronger response occurred after treatment of *pin1-1* apices with 5 mM IAA when, after 30 min, we detected an upregulation of *PIN1* by a factor of 3.2 (2.9–3.5) (Figure 2A). Although these exogenous IAA concentrations are much higher than those thought to occur physiologically, similar exogenous concentrations of IAA are required to induce a consistent growth response in both wild-type and mutant apical meristems [2, 3, 5], suggesting that high exogenous IAA concentrations applied to shoot tissues are diluted to physiologically relevant concentrations in vivo. To examine the effects of exogenous auxin on the *PIN1* expression pattern in more detail, we conducted time-lapse confocal imaging of *pPIN1::PIN1-GFP*-expressing meristems treated with 5 mM 1-naphthaleneacetic acid (NAA), a form of auxin that can diffuse into cells. We were able to detect an increase in expression beginning after 2 hr and increasing up to 6 hr post treatment in primordial cells away from which PIN1 polarity was directed, presumably after reversal (arrows, Figures 2B and 2C). Expression also increased in subepidermal cells located at primordial boundaries (arrows, Figures 2D and 2E). We also tested whether the *pPIN1::PIN1-GFP* expression pattern was sensitive to the auxin transport inhibitor N-1-naphthylphthalamic acid (NPA). After treating *pPIN1::PIN1-GFP*-expressing meristems for 6 hr with 100 μM NPA, we observed increasing delocalization of *pPIN1::PIN1-GFP* expression that by 14 hr had clearly spread to subepidermal cells surrounding the presumed vascular tissue that initially lacked expression (Figures 2F–2I). These experiments indicate that the *PIN1* expression pattern is dependent on the distribution of auxin in the meristem, which in

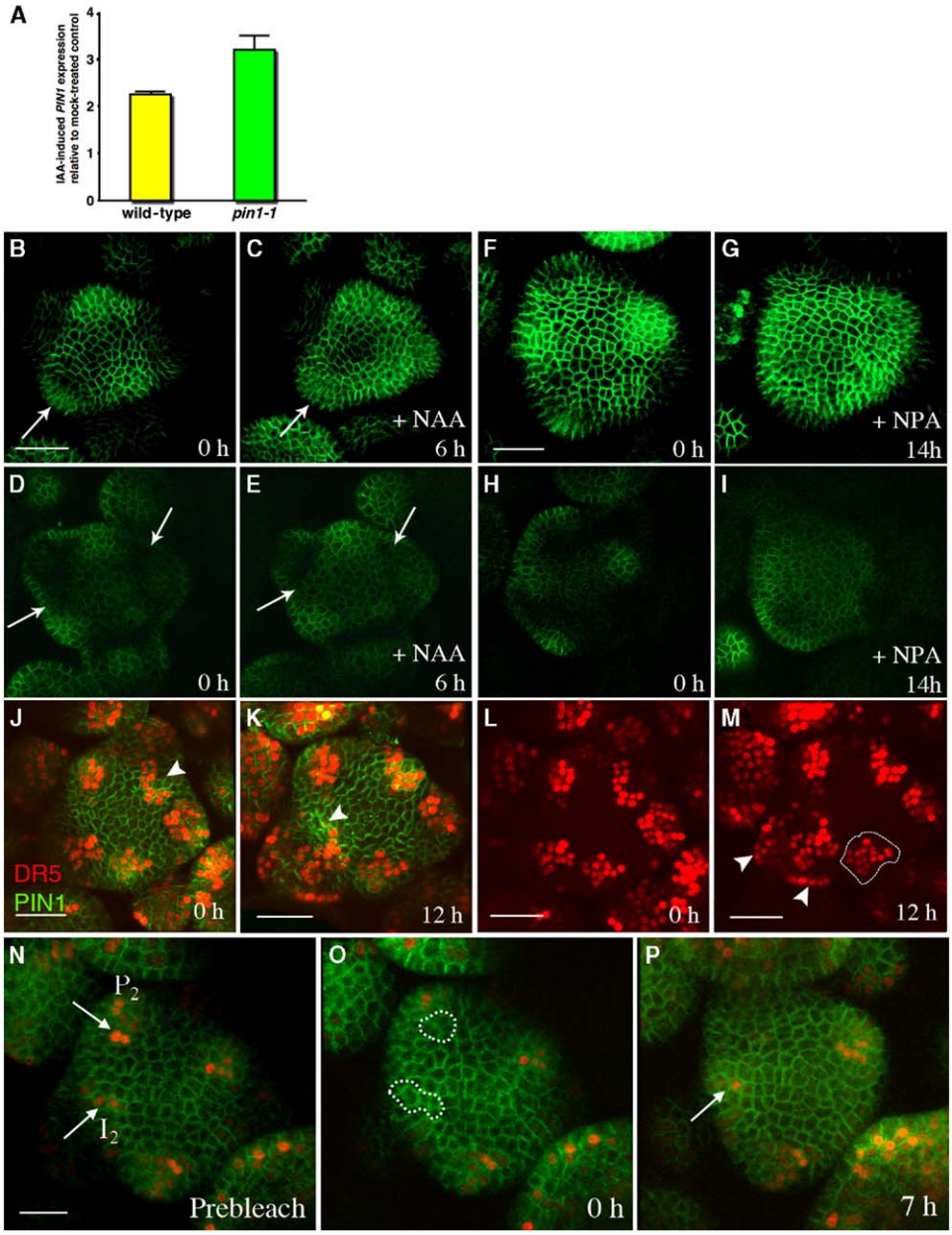

Figure 2. *PIN1* Expression Responds to Auxin

(A) *PIN1* mRNA levels as measured by real-time PCR analysis of dissected wild-type inflorescences immersed in 100 μM IAA show greater than 2-fold upregulation after 60 min relative to mock-treated controls. Identical treatments carried out on *pin1-1* mutant apices using 5 mM IAA in lanolin paste resulted in approximately 3-fold induction after 30 min. (B), (C), (F), and (G) show maximum intensity projections of the meristem viewed from above, while (D), (E), (H), and (I) show corresponding transverse optical sections below the epidermis, respectively. (B–E) Response of *pPIN1::PIN1-GFP* (green) to exogenous auxin. (B and D) *pPIN1::PIN1-GFP*-expressing meristem before NAA treatment. (C) and (E) show the same meristem as in (B) and (D) after treatment with 5 mM NAA for 6 hr. Expression becomes delocalized and increases in cells that previously expressed *pPIN1::PIN1-GFP* at low levels (arrows in [B]–[E]). This occurs both in the epidermis (compare [B] and [C]) and layers below (compare [D] and [E]). (F–I) Response of *pPIN1::PIN1-GFP* to treatment with 100 μM NPA for 14 hr. In both the epidermis (F and G) and subepidermal layers (H and I), there is a delocalization of expression after 14 hr. (J–M) Time lapse of *pDR5rev::3XVENUS-N7* (red) and *pPIN1::PIN1-GFP* (green) expression together (J and K) and *pDR5rev::3XVENUS-N7* (red) alone (L and M). At both the initial time point (J and L) and 12 hr later (K and M), *pDR5rev::3XVENUS-N7* expression initiates when *pPIN1::PIN1-GFP* expression first marks a new site (arrowheads in [J] and [K]). After *PIN1-GFP* reverses polarity in cells adaxial to primordia, primordial expression of *pDR5rev::3XVENUS-N7* persists and subsequently appears in daughter cells of earlier-expressing cells (encircled by broken line in [M]). Expression in nondaughter cells occurs at a later stage of floral bud development (arrowheads in [M]). (N and O) Recovery of fluorescence after bleaching. Cells located within incipient primordia (I_2 in [N]) and more mature primordia (P_2 in [N]) that expressed *pDR5rev::3XVENUS-N7* were selectively irradiated with 514 nm laser light until expression became undetectable (circled regions in [O]). Seven hours after bleaching, fluorescence could again be detected in the same cells at I_2 (arrow in [P]) but not in P_2. Scale bars in (B), (F), and (J)–(N), 30 μm.

turn depends on auxin transport. Since *pPIN1::PIN1-GFP* expression levels are also correlated with the observed changes in PIN1-GFP polarity, our data suggests that changes in PIN1 polarity associated with different stages of primordial development drive dynamic changes in auxin concentration, which then influence *PIN1* transcription.

To gain further evidence of a correlation between auxin concentration dynamics and PIN1 expression and polarity, we visualized the activity of the *DR5rev* auxin-responsive promoter driving three tandem copies of VENUS, a rapidly folding YFP variant [28], fused to a nuclear localization sequence, here termed *pDR5rev::3XVENUS-N7*, in combination with *pPIN1::PIN1-GFP*. As predicted, we found that local upregulation of both markers occurred simultaneously at young sites predicted to form primordia (arrowheads in Figures 2J and 2K). In contrast to *pPIN1::PIN1-GFP* expression, which decreases in primordia after PIN1-GFP polarity reverses toward the meristem in adaxial cells, *pDR5rev:3XVENUS-N7* expression persists after reversal (compare circled area in Figure 2M to corresponding region in Figure 2L). However, by time-lapse imaging, we found that these *pDR5rev::3XVENUS-N7*-expressing cells either corresponded to or were daughters of cells expressing *pDR5rev::3XVENUS-N7* before reversal (Figure 2L, circled cells in Figure 2M), suggesting the possibility that persistent expression might be due to VENUS-N7 perdurance. To test this hypothesis, we selectively radiated cells expressing *pDR5rev::3XVENUS-N7* at primordial positions with 514 nm laser light until VENUS fluorescence became undetectable. We then assessed the recovery of fluorescence in these cells over time. Of five meristems tested, three showed fluorescence recovery specifically in cells within incipient primordia but not in cells located in adjacent older primordia (Figures 2N–2P), while two plants showed no recovery at either type of position. Overall, these results support the proposal that transcription from the DR5 promoter is active during the early stages of primordial specification and that, like *pPIN1::PIN1-GFP*, DR5 expression decreases around the time that PIN1-GFP polarity reverses. De novo expression in cells unrelated to those expressing *pDR5rev::3XVENUS-N7* before PIN1-GFP reversal was detected at a later stage (arrowheads in Figure 2M), again correlated with the reappearance of *pPIN1::PIN1-GFP* expression (see also Figures 1A and 1O).

To summarize, both the *pDR5rev::3XVENUS-N7* and *pPIN1::PIN1-GFP* expression data support the proposal that reversals in PIN1 polarity correlate with and are likely to cause changes in auxin levels within developing primordia.

The Meristem Marker SHOOTMERISTEMLESS (STM) Is Downregulated as PIN1 Is Upregulated at Incipient Primordia

The *STM* gene is required both for meristem formation and maintenance [6]. In situ hybridization analysis shows that *STM* is expressed throughout most of the inflorescence meristem but is specifically downregulated at positions where specification of the cryptic floral bract is thought to occur [29]. To determine when and where STM is downregulated relative to PIN1, we visualized an *STM-VENUS* fusion protein under the control of the *STM* promoter, designated *pSTM::STM-VENUS*, in combination with *pPIN1::PIN1-GFP*. The overall expression pattern of the STM marker is similar to that found by in situ hybridization analysis with expression encompassing most of the meristem. Examination of meristems expressing both *pSTM::STM-VENUS* and *pPIN1::PIN1-GFP* reveals that *pSTM::STM-VENUS* expression is downregulated at locations where *pPIN1::PIN1-GFP* is upregulated (Figures 3A and 3B). This complementary pattern starts to become apparent at the earliest position marked by localized *pPIN1::PIN1-GFP* expression and polarity, showing that STM marks primordial positions with similar timing to PIN1 (Figures 3A and 3B). The reduction in *pSTM::STM-VENUS* expression in the vicinity of high *pPIN1::PIN1-GFP* expression is also evident several cell layers below the meristem epidermis in regions corresponding to the presumptive provascular cells (Figure 3C). We also note that *pSTM::STM-VENUS* expression strengthens in a boundary-like domain abaxial to those cells in which PIN1 is directed toward the meristem and away from the primordium (after reversal). This is most noticeable in transgenic lines in which *pSTM::STM-VENUS* expression levels are low (Figure 3F marked "b"). Lastly, we also note a reduction in *pSTM::STM-VENUS* levels toward the meristem center relative to the periphery in cells below the L2 (Figure 3C).

CUC2 Boundary Expression and PIN1 Dynamics

Previous work has shown that the *CUC1*, *CUC2*, and *CUC3* genes are required for proper organ separation [9, 10] and that, in mutants in which auxin patterning is disrupted, the expression patterns of *CUC1* and *CUC2* are also disrupted, suggesting a link between auxin patterning and *CUC* gene function [25, 30, 31].

To start to investigate the temporal and spatial relationship between the CUC genes and PIN1-mediated auxin transport patterns, we fused the *CUC2* coding region to *VENUS* and expressed it under the *CUC2* promoter, designated *pCUC2::CUC2-VENUS*, together with *pPIN1::PIN1-GFP*. *pCUC2::CUC2-VENUS* is expressed in boundary-like domains surrounding primordia in a pattern similar to that previously reported from in situ hybridization experiments [32] (Figure 3D). However, weak expression is also detected in the epidermal cells of the central zone (CZ) (arrow in Figure 3D). Like *pSTM::STM-VENUS*, we found *pCUC2::CUC2-VENUS* to be downregulated at *pPIN1::PIN1-GFP* expression and polarity foci (arrowheads in Figure 3D). This downregulation seems to occur at an earlier stage than *pSTM::STM-VENUS* and is more extensive. Like *pSTM::STM-VENUS*, *pCUC2::CUC2-VENUS* is specifically upregulated in those cells near primordia from which *pPIN1::PIN1-GFP* polarity was directed after its reversal (Figure 3E).

These data suggest that both CUC2 and STM are regulated in a similar manner, although with different timing or sensitivity. Furthermore, they show strikingly complementary expression patterns compared to PIN1 both at *pPIN1::PIN1-GFP* foci and in boundary regions from which *pPIN1::PIN1-GFP* is directed.

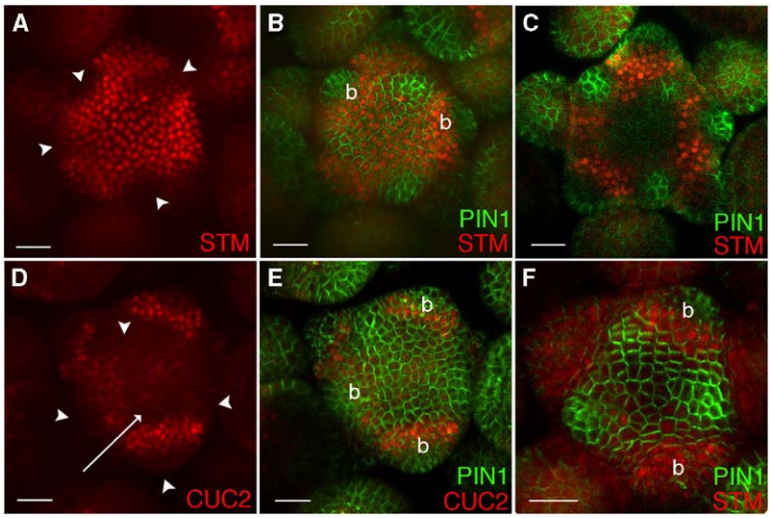

Figure 3. STM and CUC2 Expression

Both *pSTM::STM-VENUS* (red in [A]–[C] and [F]) and *pCUC2::CUC2-VENUS* (red in [D] and [E]) are expressed in a complementary domain to *pPIN1::PIN1-GFP* (green in [B], [C], [E], and [F]), with expression being absent or reduced at early positions (arrowheads in [A] and [D]) marked by *pPIN1::PIN1-GFP* polarity foci (compare [A] to [B] and [D] to [E]). However, while *pCUC2::CUC2-VENUS* expression is low in subepidermal layers (data not shown), *pSTM::STM-VENUS* is expressed at high levels in a similar pattern to its expression in the epidermis (C). After *PIN1-GFP* polarity reverses, both markers are upregulated in boundary domains (marked "b" in [B], [E], and [F]) corresponding to cells abaxial to *pPIN1::PIN1-GFP*-expressing cells exhibiting polarity away from the primordium toward the meristem. When *pSTM::STM-VENUS* expression is weak (F), its expression pattern closely resembles that of *pCUC2::CUC2-VENUS* (compare [F] to [E]). Arrow in (D) denotes weak expression. Scale bars in (A)–(C), 30 μm; in (D)–(F), 20 μm.

The Adaxial Marker REVOLUTA Is Localized after PIN1 and Remains Adaxial from Inception

The *REV* gene is involved in regulating axillary meristem formation, organ polarity, and meristem size and is expressed in a similar pattern to other related members of the HD-ZIP family of transcription factors such as *PHABULOSA* and *PHAVOLUTA* [12–14, 33–35]. It is also thought to mark primordia at a particularly young stage [13]. To monitor *REV* expression dynamics, we constructed a functional *REV-VENUS* fusion and expressed it under the *REV* promoter. We found the *pREV::REV-VENUS* transgene to be expressed in an identical manner to the reported endogenous transcription pattern [13]. *pREV::REV-VENUS* expression is present in the upper layers of the CZ of the meristem as well as in finger-like domains extending out to developing primordia (Figure 4A). *pREV::REV-VENUS* signal is first evidently associated with primordial positions between zero and one plastochron after *pPIN1::PIN1-GFP* first localizes, and the expression domain is contiguous with expression in the CZ (I_2 in Figures 4A and 4B). However, before this, newly localized *pPIN1::PIN1-GFP* expression always appears adjacent to *pREV::REV-VENUS*-expressing cells in the CZ (I_3 in Figure 4A, corresponding position in Figures 4B and 4C). As *pPIN1::PIN1-GFP* signal increases at primordial initiation sites, the *pREV::REV-VENUS* expression domain extends outward to overlap with the adaxial half of the *pPIN1::PIN1-GFP* expression domain (I_1 in Figure 4A, corresponding position in Figures 4B and 4D). This pattern of overlap also extends below the epidermis along the presumptive provascular cells marked by newly localized *pPIN1::PIN1-GFP* expression (Figure 4D). At approximately the same time that *pPIN1::PIN1-GFP* polarity reverses and expression levels decrease in subepidermal cells, *pREV::REV-VENUS* expression is lost from the cells located between the primordium and the CZ, thus isolating REV expression from the CZ (P_1 in Figure 4A, corresponding position in Figures 4B and 4E).

To summarize, *pREV::REV-VENUS* expression extends halfway into the *pPIN1::PIN1-GFP* expression domain from nearby adjacent CZ cells that already express *pREV::REV-VENUS*. Adaxial, localized *pREV::REV-VENUS* expression associated with *pPIN1::PIN1-GFP* expression is then maintained during primordial outgrowth and separation from the CZ.

The Abaxial Primordium Marker FILAMENTOUS FLOWER Is Asymmetrically Expressed at Initiation

To determine whether PIN1 expression also marks the adaxial boundary of abaxially expressed genes, we examined *pPIN1::PIN1-GFP* expression in combination with nuclear localized dsRED under the control of the *FIL* promoter. *FIL* is a member of the *YABBY* gene family of transcription factors and functions to specify abaxial cell types and to promote flower development and lateral organ expansion [15–17]. *pFIL::dsRED-N7* first marks primordia between one and two plastochrons later than upregulation of *pPIN1::PIN1-GFP* (I_1 and I_2 in Figure 4F, arrows in Figure 4G). At inception, *pFIL::dsRED-N7* expression is detected abaxial to *pPIN1::PIN1-GFP* in the two layers of cells located between the epidermis and *pPIN1::PIN1-GFP*-marked provasculature (Figure 4H). Slightly later, *pFIL::dsRED-N7* extends to the epidermis and into the *pPIN1::PIN1-GFP* expression domain (Figure 4I). At later stages, *pFIL::dsRED-N7* expression almost entirely overlaps *pPIN1::PIN1-GFP* in the primordium (Figure 4J). To investigate this more thoroughly, we covisualized *pFIL::dsRED-N7*, *pREV::REV-VENUS*, and *pPIN1::PIN1-GFP* together (represented in red, green, and blue, respectively, in Figures 4K–4O). We found that, after *pFIL::dsRED-N7* expression first expands (approximately the same stage as shown in Figure 4I), both *pREV::REV-VENUS* and *pFIL::dsRED-N7* are coexpressed in a number of cells centered within the *pPIN1::PIN1-GFP* expression domain (P_1 in Figures 4K–4O). These data confirm that both *pREV::REV-VENUS* and *pFIL::dsRED-N7* are initially expressed asymmetrically relative to *pPIN1::PIN1-GFP*, showing that *pPIN1::PIN1-GFP* marks a domain be-

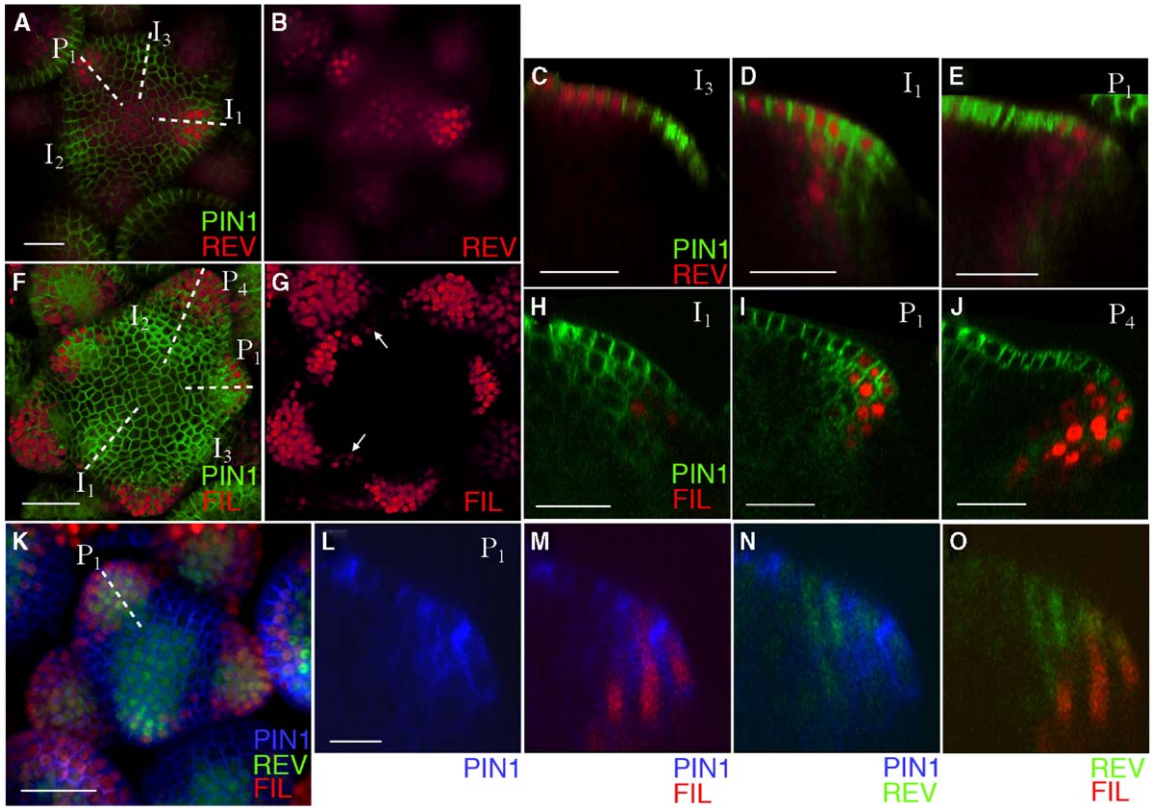

Figure 4. Relative Expression Patterns of REV, FIL, and PIN1

(C)–(E), (H)–(J), and (L)–(O) represent longitudinal sections of primordia along the planes of sections as depicted by dotted lines in (A), (F), and (K), respectively. *pREV::REV-VENUS* (red in [A]–[E]) is expressed in the CZ as well as in radial domains extending out to where *pPIN1::PIN1-GFP* (green in [A]–[J]) has established expression and polarity foci (compare [A] and [B]). *pREV::REV-VENUS* expression is localized adaxially to the first site marked by *pPIN1::PIN1-GFP* and does not overlap (I_3 in [A] and [C]). At later stages, *pREV::REV-VENUS* expression extends halfway into the cells expressing *pPIN1::PIN1-GFP* at high levels (I_1 in [A] and [D]) and later separates from the central domain of expression as subepidermal *pPIN1::PIN1-GFP* expression also becomes restricted to provascular cells (P_1 in [A] and [E]). *pFIL::dsRED-N7* (red in [F]–[O]) is expressed in primordia approximately one to two plastochrons after they are first marked by *pPIN1::PIN1-GFP* (I_1 and I_2 in [F], arrows in [G]). *pFIL::dsRED-N7* signal first appears in cells located abaxial to *pPIN1::PIN1-GFP* (I_1 in [F] and [H]) but is then found to overlap later during development (P_1 and P_4 in [I] and [J], respectively). Plants expressing all three markers (K) show that, compared to *pPINl::PIN1-GFP* (blue in [K]–[N]), both the expression patterns of *pFIL::dsRED-N7* (red) (M) and *pREV::REV-VENUS* (green) (N) are ab- and adaxially polarized within the developing primordium but also overlapping within the *pPIN1::PIN1-GFP* expression domain (O). [L]–[O] correspond to different combinations of markers expressed in the primordium P_1 in [K]. Scale bars in (A), (F), and (K), 30 μm; in (C)–(E) and (H)–(J), 20 μm; in (L), 10 μm.

tween abaxial and adaxial cell identities at primordial initiation. Soon after, as the expression domains of *REV* and *FIL* expand into the anlagen, their domains partially overlap during subsequent development.

Gene Expression Patterns during Early Initiation of Floral Development

The *LEAFY* (*LFY*) gene encodes a transcription factor involved in conferring floral meristem identity on primordia that develop from the inflorescence meristem. In *lfy* mutants, secondary inflorescence meristems subtended by floral bracts frequently develop in the place of flowers [36]. To understand where and when floral meristem identity is specified as marked by *LFY* expression, we examined the expression of the *LFY* promoter driving endoplasmic-reticulum (ER)-localized GFP in combination with *pFIL::dsRED-N7*. We detect the onset of *pLFY::GFP-ER* expression approximately two plastochrons later than *pFIL::dsRED-N7* in a few adaxial cells abutting the *pFIL::dsRED-N7* expression domain (Figures 5A and 5B). By one plastochron later, *pLFY::GFP-ER* expression is much stronger and broader, and this trend continues during later stages (Figures 5A and 5B–5D). *pLFY::GFP-ER* expression is also sharply bounded on the adaxial side of the primordium by cells predicted to express the boundary marker CUC2. If this were so, we would expect a gap to form between the FIL and CUC2 expression domains at the time LFY expression initiates. Visualization of *pCUC2::3XVENUS-N7* and *pFIL::dsRED-N7* revealed that, although the expression of these markers initially abuts (Figures 5E and 5F), later during development, a discernable gap in expression forms between their domains. This gap continues to expand during floral meristem development in a manner similar to the expansion of the *pLFY::GFP-ER* expression pattern (Figure 5H), suggesting that *LFY* expression initiates specifically in the region between the *FIL* and *CUC2* expression domains and that the *FIL*

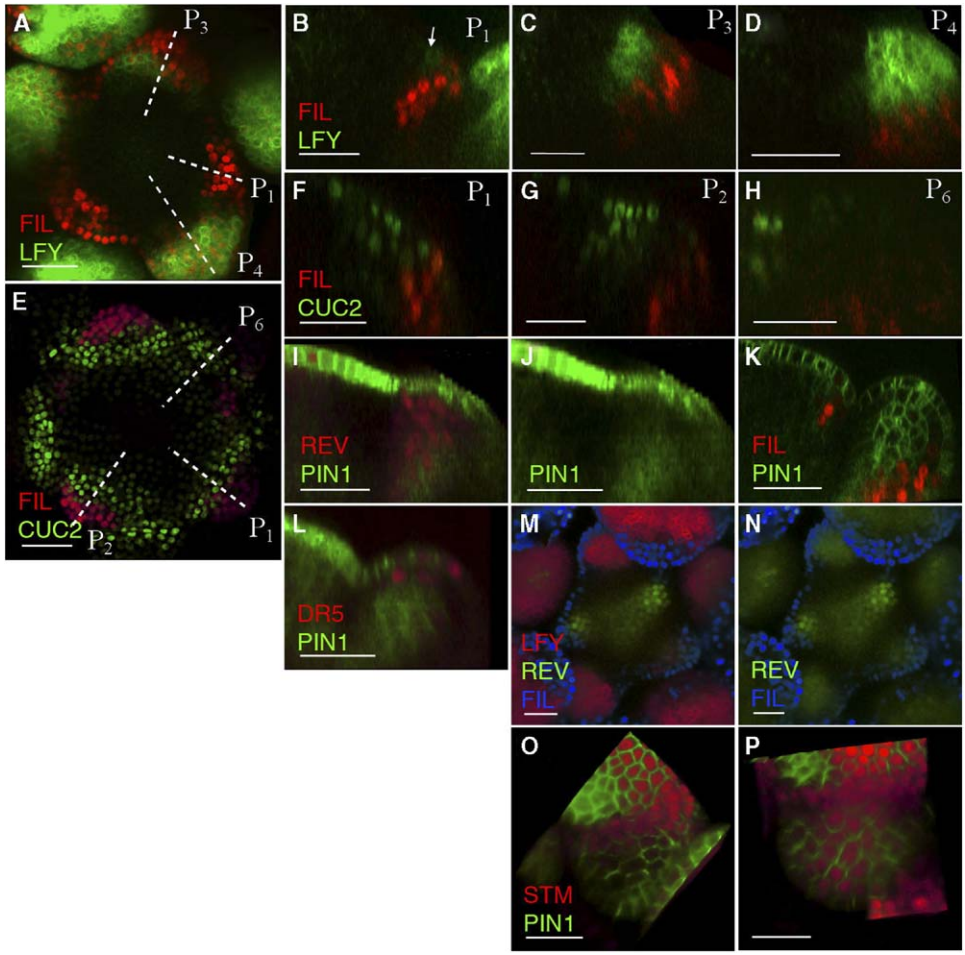

Figure 5. *pLFY::GFP-ER* Expression and the Initiation of Floral Meristem Development

(B)–(D) and (F)–(H) represent longitudinal sections along the planes of sections depicted by dotted line in (A) and (E), respectively. *pLFY::GFP-ER* (green) is initiated two plastochrons after *pFIL::dsRED-N7* (red) in a small number of cells located at the adaxial boundary of *pFIL:dsRED-N7* expression (arrow in [B]). During subsequent development, the *pLFY::GFP-ER* expression domain expands to encompass the floral meristem (B–D). (E–H) The *pCUC2::3XVENUS-N7* (green) and *pFIL::dsRED-N7* (red) domains abut each other early in primordium development (F) but become separated in a pattern complementary to the expansion of *pLFY::GFP-ER* expression (compare [A]–[D] to [E]–[H]). (I and J) During stage two of flower development, *pREV::REV-VENUS* (red) expression expands (I) as *pPIN1::PIN1-GFP* (green) also expands (J), while *pFILdsRED-N7* (red) remains restricted to the region marked by the original boundary of *pPIN1::PIN1-GFP*-expressing cells (K). (L) Also during stage two, *pDR5rev:3XVENUS-N7* expression (red) starts to reappear together with the expansion of *pPIN1::PIN1-GFP* expression (green). (M and N) *pREV::REV-VENUS* (green) and *pLFY::GFP-ER* (red) overlap during stage two. (O and P) Direction of meristem is toward the top of the pictures. During late stage two, *pSTM::STM-VENUS* expression (red) also undergoes a rapid expansion into the flower primordium from a boundary-like domain (compare [O] and [P]). Scale bars in (A), 30 μm; in (B) and (C), 20 μm; in (D) and (E), 30 μm; in (F)–(P), 20 μm.

and *CUC2* expression domains move apart, possibly through the proliferation of cells within the developing floral meristem. Since *pREV::REV-VENUS* expression also abuts *pFIL::dsRED-N7* expression, we examined *pREV::REV-VENUS* expression during stage two of flower development [27] and found that its expression also spreads adaxially in a similar manner to *pLFY:GFP-ER* (compare Figures 5C and 5I, 5M and 5N). This is further correlated with an expansion of *pPIN1::PIN1-GFP* (Figure 5J) and *pDR5rev::3XVENUS-N7* expression (Figure 5L). Although *pSTM::STM-VENUS* expression is still restricted to an adaxial boundary domain during early stage two of flower development, before stage three, *pSTM::STM-VENUS* expression also expands rapidly (compare Figures 5O and 5P).

To summarize, the *pCUC2::CUC2-VENUS* and *pFIL::dsRED-N7* expression domains are located adjacent to each other, with the boundary between these domains corresponding to the region where *pLFY::GFP-ER* expression later initiates. *pLFY::GFP-ER* expression then expands as cells proliferate to form the flower meristem, and this is correlated with an expansion of *pREV::REV-VENUS* and *pSTM::STM-VENUS* expression into the primordium as well as an increase in primordial *pDR5rev::3XVENUS-N7* expression.

Discussion

PIN1 Reversals and Primordium Positioning

Our data suggest that, within floral anlagen, there is a cycle of auxin build-up followed by decrease correlated with and likely caused by a rapid reversal in PIN1 polar-

ity in cells located adaxial to the primordium (Figure 6A). Thus, our results support the proposal that auxin is depleted from primordial regions during their development [3, 5]. However, instead of depletion occurring simply because of auxin transport into the vasculature, as previously proposed [3, 5], we show that it may result from specific reversals in PIN1 polarity away from primordia. Given this result, our data provide new insights into how PIN1 acts to position primordia. We show that upregulation of PIN1 marks anlagen first in the epidermis, suggesting that the patterning mechanism may act primarily within this cell layer, as is also suggested by laser ablation experiments [37]. We also reveal correlations between PIN1 polarity reversals at older primordia and the establishment of foci at new sites, suggesting causal links between these events. Since we find that, in the epidermis, polarity is mainly directed from older to younger sites, one possible scenario is that new sites are first specified by a reversal event at an older primordium. Such an event may be mediated by the PINOID protein kinase [38, 39], since it is expressed in boundary domains and can act as a PIN1 polarity switch [30, 40]. In accordance with this proposal, it has been known for some time that older primordia influence the position of younger primordia [37, 41, 42]. However, this hypothesis does not explain the simultaneous appearance of regularly positioned primordia in whorled phyllotaxis. Thus, an important goal for future investigation will be to determine the direction of causality between focus establishment and polarity reversal and to see how disruptions to these processes affect primordial positioning.

Boundary Establishment, Organ Specification, and PIN1 Expression

Both *STM* and *CUC* gene function are required for meristem establishment and organ separation [7, 9–11, 43]. Also, ectopic *STM* and *CUC2* expression is associated with ectopic meristem formation and abnormal development of lateral organs, indicating that tight regulation of these genes is important [8, 44, 45]. Genetic studies have also shown that PIN1 activity in the embryo is required for *CUC2* expression in cotyledon boundaries [31]. In addition, both *CUC2* and *STM* expression in the pin-like inflorescence meristem of *pin1* mutants is uniform throughout the periphery [25]. These studies suggest that both local downregulation and the specific upregulation of these genes depend on auxin transport (and therefore auxin levels) in some manner [31]. By linking *STM* and *CUC2* expression to auxin concentration and transport dynamics, we reveal how auxin transport may control these genes. We find that both *pSTM::STM-VENUS* and *pCUC2::CUC2-VENUS* are downregulated at a time when PIN1 first establishes polarity foci, coincident with a presumed auxin build-up as evidenced by *pPIN1::PIN1-GFP* and *pDR5rev::VENUS-N7* expression. Both *pCUC2::CUC2-VENUS* and *pSTM::STM-VENUS* are also upregulated in primordial boundaries at a similar time to when PIN1-GFP polarity reverses away from the primordia and apparent auxin depletion occurs in epidermal and subepidermal layers, as evidenced by PIN1 expression. Thus, there appears to be a consistent and complementary relationship between the expression of auxin reporter genes, the direction of presumed auxin flow, and the activation of *STM* and *CUC2*, suggesting that both the *STM* and *CUC2* expression domains may be patterned by the cycles of PIN1 focus establishment and reversal during primordium development (illustrated in Figure 6A). However, given the limited time resolution of this study, it is also possible that CUC2 and/or STM may act upstream of PIN1 to influence PIN1 behavior. This proposal is also suggested by the observation that upregulation of *CUC1* and *CUC2* can lead to increases in organ number [45, 46]. Further experiments testing the effect of auxin on *CUC2* and *STM* expression may help to distinguish these possibilities.

Auxin Transport Routes and the Establishment of Organ Polarity

We find that, in the inflorescence meristem, the polarity markers *pFIL::dsRED-N7* and *pREV::REV-VENUS* are expressed predominantly abaxially and adaxially, respectively, at initiation, although they overlap to some degree later on. Although this finding contrasts with some previous reports that polar expression patterns arise gradually during primordial development [12, 15], it is consistent with more recent observations showing that a mutated *FIL* promoter that drives GFP expression in both adaxial and abaxial leaf domains also drives expression more widely than the wild-type promoter during organ initiation [47]. *pREV::REV-VENUS* expression starts in the CZ completely adaxial to *pPIN1::PIN1-GFP* and then expands into, but does not completely overlap, the domain of *pPIN1::PIN1-GFP*-marked cells. In contrast, *pFIL::dsRED-N7* appears to be initiated in cell layers lying in between *pPIN1::PIN1-GFP*-marked cells and the epidermis, although its domain quickly expands to almost completely encompass the *pPIN1::PIN1-GFP* domain (summarized in Figure 6B). These results show that, in flower primordia, polarity is established at least as early as the onset of *REV* and *FIL* expression. It is also intriguing to note that *pPIN1::PIN1-GFP* marks the abaxial boundary of *pREV::REV-VENUS* expression. This suggests that, in addition to specifying primordial positions and boundary domains (as defined by CUC2 and STM expression), auxin transport routes also play a role in positioning boundaries between adaxial and abaxial cell types.

Early Development of the *Arabidopsis* Flower

Our results indicate that *LFY* expression arises in a boundary region between the *CUC2* (and presumably *STM*) and *FIL* expression domains. From our analysis of *pFIL::dsRED-N7* and *pPIN1::PIN1-GFP*, this region also corresponds to cells marked by PIN1, suggesting yet another role for auxin transport routes in either directly or indirectly positioning *LFY* expression and thus influencing floral development. During subsequent stages, this domain undergoes significant expansion. From our observations, it appears that, during this expansion, the *FIL* and *CUC2* expression domains do not become reduced, suggesting either that their expression domains are moving relative to the *LFY*-expressing cells or that the *LFY* domain is undergoing rapid growth such that the *CUC2* and *FIL* domains are physically pushed apart (see Figure 6B). The latter proposal is supported by previous work showing that, although *LFY* expression initi-

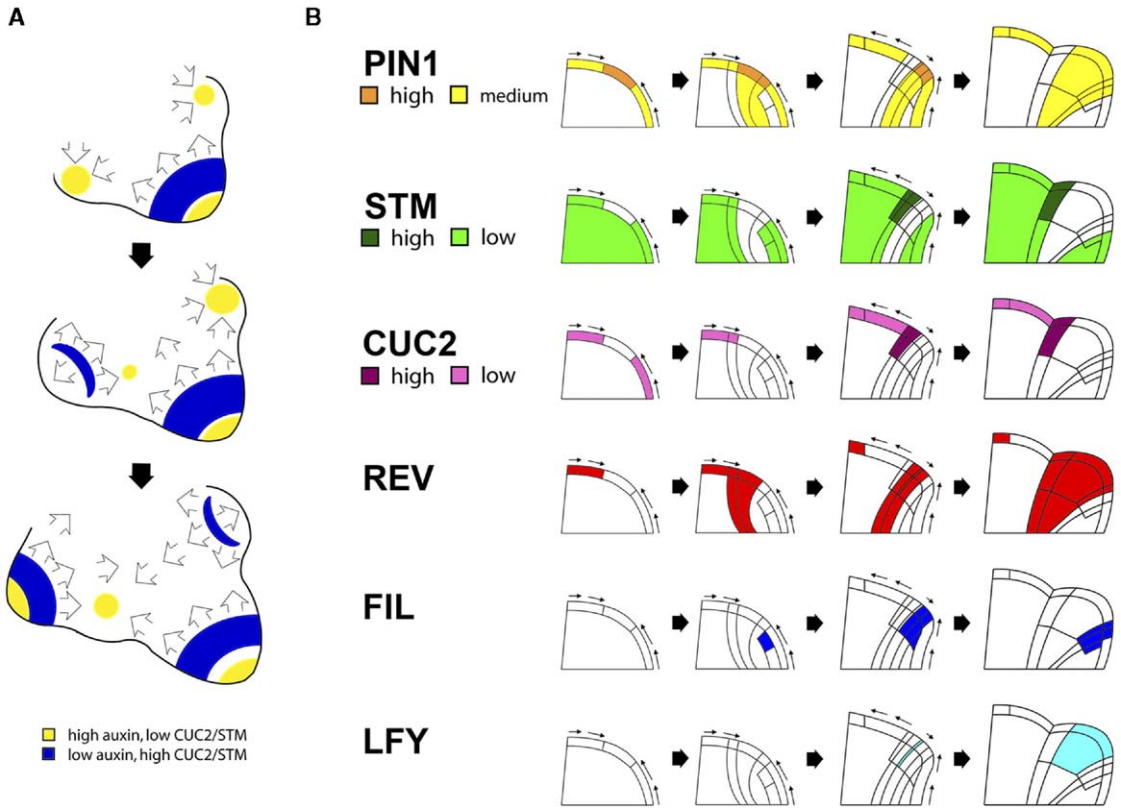

Figure 6. Conceptual Summary

(A) PIN1 polarity (arrows), presumed auxin concentration dynamics, and CUC2/STM expression levels. High auxin, low STM/CUC2 (yellow); low auxin, high STM/CUC2 (blue).

(B) Summary of observed expression patterns during early stages of primordial development. Arrows indicated direction of auxin transport in the epidermis.

ates first by cell recruitment, this is later followed by expansion through cell proliferation [23]. That LFY may in fact be required for such growth is suggested by the reduced size of floral meristems that arise in *lfy* mutants [36]. Lastly, it is worth noting that, at the time when *pLFY::GFP-ER* expression expands, we also see the reappearance of *pDR5rev::3XVENUS-N7* expression and a widening and strengthening of *pPIN1::PIN1-GFP* and *pREV::REV-VENUS*. Slightly later, *pSTM::STM-VENUS* expression also expands. These events presumably indicate the onset of floral meristem activity.

Conclusion

Besides determining primordial position, auxin transport patterns play a crucial role in other developmental processes including venation patterning [48, 49], establishing the embryo apical-basal axis [50], promoting differential growth in response to gravity [51], and formation of the root meristem [40, 52–54]. Our study shows that this patterning system also potentially acts to influence later differentiation events that occur during flower primordium formation, including boundary formation, organ polarity, and floral meristem initiation. Thus, auxin transport routes may provide positional information for many developmental processes throughout the plant life cycle. An important goal for future investigation will be to test our causal hypotheses and understand the mechanisms that determine the transport routes themselves.

Experimental Procedures

Construction of GFP Reporters

The *pPIN1::PIN1-GFP* fusion construct was made by inserting mGFP5 (a gift from J. Hasseloff) into a unique XhoI site located in a 8763 bp genomic DNA fragment obtained by PCR containing the PIN1 gene (3506 bp upstream of ATG to 2181 bp downstream of the stop codon). This fragment was then transformed into plants heterozygous for the *pin1-4* mutation using the pART27 binary transformation vector [55]. Functionality was confirmed by identifying several T3 families in which the wild-type phenotype strictly cosegregated with the transgene. *3XVENUS-N7* was constructed by first PCR amplifying both VENUS [27] and N7, a DNA-fragment-encoding nuclear-localization protein sequence [56], with restriction sites and cloning them in frame to yield BamHI-VENUS-4Xala-N7-XbaI (pPD19). The BamHI-XbaI fragment from pPD19 was then subcloned to pBJ36 [28] to yield pPD31. Separately, VENUS was also PCR amplified and cloned to pCR2.1-TOPO, flanked by BamHI and BglII sites (pPD30). The BamHI-BglII fragment from pPD30 was then ligated to BamHI-linearized pPD31 and screened for clones with multiple insertions to yield 3XVENUS-4XAlanine-N7 (pPD35). *pDR5rev::3XVENUS-N7* was constructed by cloning the DR5rev promoter [50] upstream of the *3XVENUS-N7* coding region, and a NotI fragment containing the reporter construct was then transfer-

red to pMLBART [57] and transformed into *pPIN1::PIN1-GFP*-expressing plants. For constructing both the *pSTM::STM-VENUS*- and *pREV::REV-VENUS*-translational fusions, a version of BJ36 containing a 9X Alanine linker followed by VENUS was made. For STM, a full-length *STM* cDNA was cloned and inserted in-frame next to the Alanine linker. A 5.76 kb region of upstream regulatory sequence was then inserted upstream of the cDNA. A NotI fragment containing this reporter was cloned into pMLBART and transformed into *pPIN1::PIN1-GFP* as described above. The ability of this construct to rescue the *stm* mutant phenotype has not been tested. *pREV::REV-VENUS* was constructed by amplifying a 7972 bp genomic DNA fragment containing 3779 bp of sequence upstream of the ATG as well as the whole genomic coding region into BJ36 containing 9X Alanine VENUS and transformed into Landsberg *erecta* plants expressing *pPIN1::PIN1-GFP* and *rev-1* homozygous mutants. Although the phenotype of transformed *rev-1* plants was variable, many selected T1 plants exhibited a wild-type phenotype. We used a CUC2 promoter reporter consisting of 3.2 kb of 5′ regulatory region fused to the 3XVENUS-N7 reporter as described above. *pCUC2::CUC2-VENUS* was constructed by switching both the CaMV 35S promoter for the 3.2 kb CUC2 upstream regulatory sequence and VENUS for mGFP5 in a previously reported 35S*::CUC2-GFP* construct [45]. Subsequently, a 9X Alanine linker was introduced as a translational fusion into the PstI site between CUC2 and VENUS and transformed as described above. Functionality of this fusion protein has not been tested. The *pFIL::dsRED-N7* marker was constructed by fusing dsRED Express (Clontech) to the nuclear localizing sequence N7 as described for VENUS-N7 above. DNA (5867 bp) upstream of the ATG start was then cloned upstream of dsRED-N7 in BJ36 and transformed into *pPIN1::PIN1-GFP*-expressing plants as described above. *pLFY::GFP-ER* was made by amplifying a 2288 bp fragment upstream of the LFY coding region and inserting it upstream of the mGFP5-ER coding region (a gift from J. Hasseloff) in the pZP222 vector [58].

Auxin Treatments

For quantitative real-time PCR analysis, inflorescences were dissected and older flowers removed. The inflorescences were then submerged in either 1% dimethylsulfoxide (DMSO) or 100 μM IAA (Sigma) dissolved in 1% DMSO. For treatment of *pin1-1* apices, an auxin paste was applied made from 5 mM IAA, 1% DMSO in lanolin (Sigma), or a mock treatment of 1% DMSO in lanolin. For live imaging, we found that 1% DMSO alone altered PIN1::GFP expression, and so both IAA and NAA (Sigma) were dissolved in 1 M KOH to make 0.5 M IAA or NAA stock, which was then diluted to 5 mM in H_2O. A 1 M stock of NPA (Chem Service) dissolved in DMSO was diluted in H_2O to give a 100 μM treatment solution. Approximately 10 μl of solution was added to the meristem after each imaging session every 2 hr. Each treatment experiment was repeated at least three times with mock treatment controls.

Quantitative Real-Time PCR

Total RNA was extracted using RNAeasy columns (QIAGEN) and subjected to on-column DNase treatment according to the manufacturer's instructions. RNA (1 μg) was then reverse transcribed using oligo dT (20-mer) and SuperScript II Rnase H Reverse Transcriptase (Invitrogen) according to the manufacturer's instructions. The reaction mixture was diluted to 30 μl, and 1 μl was used per real-time PCR reaction. Each primer pair was designed to cross introns in order to eliminate the possibility of genomic DNA amplification. The primers for *PIN1* were 5′-ACAAAACGACGCAGGC TAAG-3′ and 5′-AGCTGGCATTTCAATGTTCC-3′. We used both the *ACTIN2* and *ACTIN8* genes as internal controls by using the following primers that amplify both genes 5′-GGTAACATTGTGCTCAG TGGTGG-3′ and 5′-AACGACCTTAATCTTCATGCTGC-3′(3). Each PCR reaction contained 12.5 μl of SYBR Green PCR Master kit containing Hot Start *Taq* polymerase (Perkin-Elmer Applied Biosystems), 3 μl of 2.5 μM primers, 1 μl of cDNA, and 7.5 μl of H_20 for a reaction volume of 25 μl. Reactions were performed in triplicate on a GeneAmp 7500 thermocycler (Perkin-Elmer Applied Biosystems). Data was analyzed using the $2^{-\Delta\Delta CT}$ method [59]. The amplification efficiencies for the *ACTIN2/8* and *PIN1* primers were found to be approximately equal. The data were collected from three independent treatments and are expressed as a mean fold change and range in brackets corresponding to the mean $-\Delta\Delta C_T \pm$ SEM converted to a fold-change value.

Tissue Preparation for Confocal Analysis

Inflorescence meristems were prepared for live imaging as described [22]. L*er* plants expressing the GFP markers were generated by transforming a chosen *pPIN1::PIN1-GFP*-transgenic line with all other markers. Triple-marker combinations were generated by crossing the double-marker plants and screening the F2 families. For high-resolution images, fixed stained tissue was prepared by applying 10 μg ml^{-1} FM4-64 (Molecular Probes) to intact inflorescences. After 30 min, inflorescences were detached and fixed in 4% paraformaldehyde containing 0.1% Tween 20 and 0.1% Triton X-100 at 4°C for 1 hr. For whole mounts, mature buds were dissected away and the meristem immersed in 50% glycerol under a coverslip ready for imaging using a Zeiss Plan-Apochromat 63×/1.40 NA objective.

Confocal Settings for GFP Combinations

All imaging was done using a Zeiss 510LSM Meta using a water-dipping 63× objective with the plant temporarily under water. For time-lapse imaging of GFP alone, we used a 488 nm laser line together with a HFT KP 650 (short-pass) main dichroic and a 505 nm long-pass filter. The laser was attenuated to 7%, and we used 0.7 s scans of a 512 × 512 pixel frame. Stacks of 30 sections spaced approximately 1.5 μm apart were collected every 2 hr. In between imaging, the water was decanted and the boxes containing the plants placed in a growth cabinet. Non-time-lapse images of GFP alone were collected as above, except we used a 505–550 nm band-pass filter and a higher laser setting and smaller pinhole. To image GFP and dsRED together, we used multitracking in line-scan mode and a 488/543 main dichroic. We used a 545 secondary dichroic to split the emission in conjunction with a 543 nm laser line and 560–610 nm band-pass filter for dsRED, and the 488 nm laser line and a 505–550 nm band pass filter for GFP. The conditions for imaging GFP/VENUS combinations depended on the relative strengths of the markers. For strong VENUS with GFP, both fluorescent proteins were excited using the 488 nm laser line, and the emission was separated using the Meta spectral analyser. For weaker VENUS signal, we used multitracking in frame mode. VENUS was excited using the 514 nm laser line in conjunction with a 530–600 band-pass filter. GFP was excited with the 477 nm laser line and collected using a 545 secondary dichroic in conjunction with a 505–530 band-pass filter. For triple combinations of GFP, VENUS, and dsRED, we used frame multitracking. The settings were as for GFP/VENUS multitracking except with an additional track for dsRED using the 543 nm laser line in conjunction with a 543 secondary dichroic to separate the excitation light and 560–610 band-pass filter.

Bleaching Experiments

Images of five meristems were recorded prior to bleaching. Then, using the Zeiss LSM software, two regions of interest corresponding to *pDR5rev::3XVENUS-N7*-expressing cells located in incipient and older primordia were selected in each of the meristems. These regions were then continuously scanned using the 514 nm laser line at 80% power until signal could not be detected using the settings initially used for imaging the prebleached meristem. After allowing 7 hr for recovery, we reimaged the meristems to assess fluorescence recovery.

Image Analysis and Assessment of PIN1-GFP Polarity

Visualization of volume renderings was performed using Zeiss LSM software and Amira (Mercury Computer Systems). At high resolution, the subcellular localization of PIN1-GFP could be assessed either by direct visualization or by analysis with image-processing software specifically developed for this purpose (H. Jonsson, M.G.H., B. Shapiro, E.M.M., and E. Mjolsness, unpublished data). Analysis of meristems imaged in this manner confirms that, in general, arcs of signal visible in approximately two thirds of meristem epidermal cells at lower resolution in 3D projections corresponded to PIN1-GFP protein localization within cell corners as shown in

Figure S1. 3D projections give a clearer indication of lateral subcellular PIN1-GFP polarity in the meristem compared to 2D optical transverse sections because the viewing angle can be manipulated to be normal to the curved epidermal surface. The pattern of PIN1-GFP polarity and expression associated with different stages of primordium development shown in Figure 1 was representative of data gathered from greater than 50 plants, as assessed visually.

Supplemental Data

Supplemental Data include two figures and two movies and can be found with this article online at http://www.current-biology.com/cgi/content/full/15/21/1899/DC1/.

Acknowledgments

We are grateful to members of the Meyerowitz laboratory for critical comments and suggestions for the manuscript. We thank Jan Traas for communicating unpublished results. This work was supported by Department of Energy grant DOE FG02-88ER13873 and National Science Foundation grant FIBR 0330786.

Received: August 11, 2005
Revised: September 27, 2005
Accepted: September 27, 2005
Published: November 7, 2005

References

1. Okada, K., Ueda, J., Komaki, M.K., Bell, C.J., and Shimura, Y. (1991). Requirement of the auxin polar transport system in early stages of *Arabidopsis* floral bud formation. Plant Cell *3*, 677–684.
2. Reinhardt, D., Mandel, T., and Kuhlemeier, C. (2000). Auxin regulates the initiation and radial position of plant lateral organs. Plant Cell *12*, 507–518.
3. Reinhardt, D., Pesce, E.R., Stieger, P., Mandel, T., Baltensperger, K., Bennett, M., Traas, J., Friml, J., and Kuhlemeier, C. (2003). Regulation of phyllotaxis by polar auxin transport. Nature *426*, 255–260.
4. Benkova, E., Michniewicz, M., Sauer, M., Teichmann, T., Seifertova, D., Jurgens, G., and Friml, J. (2003). Local, efflux-dependent auxin gradients as a common module for plant organ formation. Cell *115*, 591–602.
5. Stieger, P.A., Reinhardt, D., and Kuhlemeier, C. (2002). The auxin influx carrier is essential for correct leaf positioning. Plant J. *32*, 509–517.
6. Endrizzi, K., Moussian, B., Haecker, A., Levin, J.Z., and Laux, T. (1996). The SHOOT MERISTEMLESS gene is required for maintenance of undifferentiated cells in *Arabidopsis* shoot and floral meristems and acts at a different regulatory level than the meristem genes WUSCHEL and ZWILLE. Plant J. *10*, 967–979.
7. Long, J.A., Moan, E.I., Medford, J.I., and Barton, M.K. (1996). A member of the KNOTTED class of homeodomain proteins encoded by the STM gene of Arabidopsis. Nature *379*, 66–69.
8. Lenhard, M., Jurgens, G., and Laux, T. (2002). The WUSCHEL and SHOOTMERISTEMLESS genes fulfil complementary roles in *Arabidopsis* shoot meristem regulation. Development *129*, 3195–3206.
9. Aida, M., Ishida, T., Fukaki, H., Fujisawa, H., and Tasaka, M. (1997). Genes involved in organ separation in *Arabidopsis*: an analysis of the cup-shaped cotyledon mutant. Plant Cell *9*, 841–857.
10. Vroemen, C.W., Mordhorst, A.P., Albrecht, C., Kwaaitaal, M.A., and de Vries, S.C. (2003). The CUP-SHAPED COTYLEDON3 gene is required for boundary and shoot meristem formation in *Arabidopsis*. Plant Cell *15*, 1563–1577.
11. Takada, S., Hibara, K., Ishida, T., and Tasaka, M. (2001). The CUP-SHAPED COTYLEDON1 gene of *Arabidopsis* regulates shoot apical meristem formation. Development *128*, 1127–1135.
12. McConnell, J.R., Emery, J., Eshed, Y., Bao, N., Bowman, J., and Barton, M.K. (2001). Role of PHABULOSA and PHAVOLUTA in determining radial patterning in shoots. Nature *411*, 709–713.
13. Otsuga, D., DeGuzman, B., Prigge, M.J., Drews, G.N., and Clark, S.E. (2001). REVOLUTA regulates meristem initiation at lateral positions. Plant J. *25*, 223–236.
14. Emery, J.F., Floyd, S.K., Alvarez, J., Eshed, Y., Hawker, N.P., Izhaki, A., Baum, S.F., and Bowman, J.L. (2003). Radial patterning of *Arabidopsis* shoots by class IIIHD-ZIP and KANADI genes. Curr. Biol. *13*, 1768–1774.
15. Siegfried, K.R., Eshed, Y., Baum, S.F., Otsuga, D., Drews, G.N., and Bowman, J.L. (1999). Members of the YABBY gene family specify abaxial cell fate in *Arabidopsis*. Development *126*, 4117–4128.
16. Chen, Q., Atkinson, A., Otsuga, D., Christensen, T., Reynolds, L., and Drews, G.N. (1999). The *Arabidopsis* FILAMENTOUS FLOWER gene is required for flower formation. Development *126*, 2715–2726.
17. Sawa, S., Watanabe, K., Goto, K., Liu, Y.G., Shibata, D., Kanaya, E., Morita, E.H., and Okada, K. (1999). FILAMENTOUS FLOWER, a meristem and organ identity gene of *Arabidopsis*, encodes a protein with a zinc finger and HMG-related domains. Genes Dev. *13*, 1079–1088.
18. Eshed, Y., Izhaki, A., Baum, S.F., Floyd, S.K., and Bowman, J.L. (2004). Asymmetric leaf development and blade expansion in *Arabidopsis* are mediated by KANADI and YABBY activities. Development *131*, 2997–3006.
19. Kerstetter, R.A., Bollman, K., Taylor, R.A., Bomblies, K., and Poethig, R.S. (2001). KANADI regulates organ polarity in *Arabidopsis*. Nature *411*, 706–709.
20. Kidner, C.A., and Martienssen, R.A. (2004). Spatially restricted microRNA directs leaf polarity through ARGONAUTE1. Nature *428*, 81–84.
21. Sussex, I.M. (1955). Morphogenesis in *Solanum tuberosum* l: experimental investigation of leaf dorsiventrality and orientation in the juvenile shoot. Phytomorphology *5*, 286–300.
22. Reddy, G.V., Heisler, M.G., Ehrhardt, D.W., and Meyerowitz, E.M. (2004). Real-time lineage analysis reveals oriented cell divisions associated with morphogenesis at the shoot apex of *Arabidopsis thaliana*. Development *131*, 4225–4237.
23. Grandjean, O., Vernoux, T., Laufs, P., Belcram, K., Mizukami, Y., and Traas, J. (2004). In vivo analysis of cell division, cell growth, and differentiation at the shoot apical meristem in arabidopsis. Plant Cell *16*, 74–87.
24. Berg, R.H. (2004). Evaluation of spectral imaging for plant cell analysis. J. Microsc. *214*, 174–181.
25. Vernoux, T., Kronenberger, J., Grandjean, O., Laufs, P., and Traas, J. (2000). PIN-FORMED 1 regulates cell fate at the periphery of the shoot apical meristem. Development *127*, 5157–5165.
26. Galweiler, L., Guan, C., Muller, A., Wisman, E., Mendgen, K., Yephremov, A., and Palme, K. (1998). Regulation of polar auxin transport by AtPIN1 in *Arabidopsis* vascular tissue. Science *282*, 2226–2230.
27. Smyth, D.R., Bowman, J.L., and Meyerowitz, E.M. (1990). Early flower development in *Arabidopsis*. Plant Cell *2*, 755–767.
28. Nagai, T., Ibata, K., Park, E.S., Kubota, M., Mikoshiba, K., and Miyawaki, A. (2002). A variant of yellow fluorescent protein with fast and efficient maturation for cell-biological applications. Nat. Biotechnol. *20*, 87–90.
29. Long, J., and Barton, M.K. (2000). Initiation of axillary and floral meristems in *Arabidopsis*. Dev. Biol. *218*, 341–353.
30. Furutani, M., Vernoux, T., Traas, J., Kato, T., Tasaka, M., and Aida, M. (2004). PIN-FORMED1 and PINOID regulate boundary formation and cotyledon development in *Arabidopsis* embryogenesis. Development *131*, 5021–5030.
31. Aida, M., Vernoux, T., Furutani, M., Traas, J., and Tasaka, M. (2002). Roles of PIN-FORMED1 and MONOPTEROS in pattern formation of the apical region of the *Arabidopsis* embryo. Development *129*, 3965–3974.
32. Ishida, T., Aida, M., Takada, S., and Tasaka, M. (2000). Involvement of CUP-SHAPED COTYLEDON genes in gynoecium and ovule development in *Arabidopsis thaliana*. Plant Cell Physiol. *41*, 60–67.
33. Prigge, M.J., Otsuga, D., Alonso, J.M., Ecker, J.R., Drews, G.N., and Clark, S.E. (2005). Class III homeodomain-leucine zipper gene family members have overlapping, antagonistic, and distinct roles in *Arabidopsis* development. Plant Cell *17*, 61–76.

34. Zhong, R., and Ye, Z.H. (2001). Alteration of auxin polar transport in the *Arabidopsis* ifl1 mutants. Plant Physiol. *126*, 549–563.
35. Talbert, P.B., Adler, H.T., Parks, D.W., and Comai, L. (1995). The REVOLUTA gene is necessary for apical meristem development and for limiting cell divisions in the leaves and stems of *Arabidopsis thaliana*. Development *121*, 2723–2735.
36. Weigel, D., Alvarez, J., Smyth, D.R., Yanofsky, M.F., and Meyerowitz, E.M. (1992). Leafy controls floral meristem identity in *Arabidopsis*. Cell *69*, 843–859.
37. Reinhardt, D., Frenz, M., Mandel, T., and Kuhlemeier, C. (2003). Microsurgical and laser ablation analysis of interactions between the zones and layers of the tomato shoot apical meristem. Development *130*, 4073–4083.
38. Benjamins, R., Quint, A., Weijers, D., Hooykaas, P., and Offringa, R. (2001). The PINOID protein kinase regulates organ development in *Arabidopsis* by enhancing polar auxin transport. Development *128*, 4057–4067.
39. Christensen, S.K., Dagenais, N., Chory, J., and Weigel, D. (2000). Regulation of auxin response by the protein kinase PINOID. Cell *100*, 469–478.
40. Friml, J., Yang, X., Michniewicz, M., Weijers, D., Quint, A., Tietz, O., Benjamins, R., Ouwerkerk, P.B.F., Ljung, K., Sandberg, G., et al. (2004). A PINOID-dependent binary switch in apical-basal PIN polar targeting directs auxin efflux. Science *306*, 862–865.
41. Reinhardt, D., Frenz, M., Mandel, T., and Kuhlemeier, C. (2005). Microsurgical and laser ablation analysis of leaf positioning and dorsoventral patterning in tomato. Development *132*, 15–26.
42. Snow, M.S., and Snow, R. (1931). Experiments on phyllotaxis I. The effect of isolating a primordium. Philos. Trans. R. Soc. Lond. B Biol. Sci. *221*, 1–43.
43. Aida, M., Ishida, T., and Tasaka, M. (1999). Shoot apical meristem and cotyledon formation during *Arabidopsis* embryogenesis: interaction among the CUP-SHAPED COTYLEDON and SHOOT MERISTEMLESS genes. Development *126*, 1563–1570.
44. Daimon, Y., Takabe, K., and Tasaka, M. (2003). The CUP-SHAPED COTYLEDON genes promote adventitious shoot formation on calli. Plant Cell Physiol. *44*, 113–121.
45. Baker, C.C., Sieber, P., Wellmer, F., and Meyerowitz, E.M. (2005). The *early extra petals1* mutant uncovers a role for microRNA miR164c in regulating petal number in *Arabidopsis*. Curr. Biol. *15*, 303–315.
46. Mallory, A.C., Dugas, D.V., Bartel, D.P., and Bartel, B. (2004). MicroRNA regulation of NAC-domain targets is required for proper formation and separation of adjacent embryonic, vegetative, and floral organs. Curr. Biol. *14*, 1035–1046.
47. Watanabe, K., and Okada, K. (2003). Two discrete cis elements control the abaxial side-specific expression of the FILAMENTOUS FLOWER gene in *Arabidopsis*. Plant Cell *15*, 2592–2602.
48. Sachs, T. (1981). The control of the patterned differentiation of vascular tissues. Adv. Bot. Res. *9*, 151–162.
49. Sieburth, L.E. (1999). Auxin is required for leaf vein pattern in *Arabidopsis*. Plant Physiol. *121*, 1179–1190.
50. Friml, J., Vieten, A., Sauer, M., Weijers, D., Schwarz, H., Hamann, T., Offringa, R., and Jurgens, G. (2003). Efflux-dependent auxin gradients establish the apical-basal axis of *Arabidopsis*. Nature *426*, 147–153.
51. Friml, J., Wisniewska, J., Benkova, E., Mendgen, K., and Palme, K. (2002). Lateral relocation of auxin efflux regulator PIN3 mediates tropism in *Arabidopsis*. Nature *415*, 806–809.
52. Blilou, I., Xu, J., Wildwater, M., Willemsen, V., Paponov, I., Friml, J., Heidstra, R., Aida, M., Palme, K., and Scheres, B. (2005). The PIN auxin efflux facilitator network controls growth and patterning in *Arabidopsis* roots. Nature *433*, 39–44.
53. Friml, J., Benkova, E., Blilou, I., Wisniewska, J., Hamann, T., Ljung, K., Woody, S., Sandberg, G., Scheres, B., Jurgens, G., et al. (2002). AtPIN4 mediates sink-driven auxin gradients and root patterning in *Arabidopsis*. Cell *108*, 661–673.
54. Aida, M., Beis, D., Heidstra, R., Willemsen, V., Blilou, I., Galinha, C., Nussaume, L., Noh, Y.S., Amasino, R., and Scheres, B. (2004). The PLETHORA genes mediate patterning of the *Arabidopsis* root stem cell niche. Cell *119*, 109–120.
55. Gleave, A.P. (1992). A versatile binary vector system with a T-DNA organisational structure conducive to efficient integration of cloned DNA into the plant genome. Plant Mol. Biol. *20*, 1203–1207.
56. Cutler, S.R., Ehrhardt, D.W., Griffitts, J.S., and Somerville, C.R. (2000). Random GFP: cDNA fusions enable visualization of subcellular structures in cells of *Arabidopsis* at a high frequency. Proc. Natl. Acad. Sci. USA *97*, 3718–3723.
57. Eshed, Y., Baum, S.F., Perea, J.V., and Bowman, J.L. (2001). Establishment of polarity in lateral organs of plants. Curr. Biol. *11*, 1251–1260.
58. Hajdukiewicz, P., Svab, Z., and Maliga, P. (1994). The small, versatile pPZP family of Agrobacterium binary vectors for plant transformation. Plant Mol. Biol. *25*, 989–994.
59. Livak, K.J., and Schmittgen, T.D. (2001). Analysis of relative gene expression data using real-time quantitative PCR and the 2(–Delta Delta C(T)) method. Methods *25*, 402–408.